

Chemical bond elongation following core-excitation of ammonia: Resonant Auger spectra calculation

Osamu Takahashi*, Kodai Matsuyama, Kiyohiko Tabayashi, and Katsuyoshi Yamazaki
Department of Chemistry, Hiroshima University, Higashi-Hiroshima 739-8526, Japan

e-mail: shu@hiroshima-u.ac.jp

Abstract. Theoretical resonant Auger decay spectra of ammonia with core-hole excited state dynamics simulation were investigated and some specific features of the experiment except for a vibrational structure were reproduced. A power spectral analysis with short-time maximum entropy method has been applied, and an obtained vibrational spacing assigned to NH stretching mode was 340 meV, which was consistent with the experiment of 390 ± 10 meV. Proton dynamics of ammonia on the first core-excited state was discussed.

1. Introduction

Auger decay [1, 2] is one of the de-excitation processes in atoms and molecules after core-excitation. The processes are classified based on the excitation energy as "normal" or "resonant" Auger decay for autoionization of a state created through ionization of an inner-shell electron and through resonant excitation of an inner-shell electron to an unoccupied valence orbital. Depending on the potential energy surface of the excited state the molecule may undergo dynamics during the core-hole lifetime, which depends on the specific element and is in the range of femtoseconds for the second-row atoms. Even if the core-excited state is dissociative, the Auger decay transition in most cases takes place before a bond scission. For some special cases, however, the repulsive character of the potential energy surface in the core-excited state can induce bond scissions within the core-hole lifetime; this is usually referred to as ultra-fast dissociation. Ultra-fast dissociation upon resonant core-excitation into dissociative states has indeed been observed by several researchers through effects on the subsequent Auger decay [3-8] and X-ray emission [9-11].

The ammonia molecule is the simplest molecule including an N atom and has been studied for a long time experimentally and theoretically. It is also interested from a viewpoint of periodicity because HF, H₂O, NH₃, and CH₄ are isoelectronic with neon. Recent developments of soft X-ray

spectroscopy have been realized detailed dynamics and electronic structure of ammonia [8, 12-16]. For instance, Schirmer et al. discussed that the $4a_1$ orbital to be nonbonding, with relatively small coupling constants for both totally symmetric vibrational modes [12]. And they also discussed that a peak of X-ray absorption spectra by $N(1s) \rightarrow 4a_1$ excitation narrows for the deuterated isotope due to a strong unresolved H-N-H bending mode excitation combined with the Jahn-Teller instability. Previously, we reported Auger decay calculations with core-hole excited state molecular dynamics (CHES MD) simulations of water [17]. In the case of water, a core-excitation into the anti-bonding $4a_1$ orbital induces ultra-fast proton dynamics due to a strong OH anti-bonding potential energy surface, seen as a signature of OH + H fragments in the Auger spectra in the gas phase [7]. Furthermore, resonant Auger decay spectroscopy of ammonia has been investigated by the same group [8]. In this case, an observed vibrational progression was assigned as a vibrational mode of NH_2 which is one of fragment molecules and an evidence of the ultra-fast dissociation.

In the present study our theoretical procedure is applied to the resonant Auger spectra based on *ab initio* CHES MD simulations to analyze a dissociation process of ammonia. A quantum dynamical treatment in terms of a pre-calculated potential energy surface necessarily involves a reduction of dimensionality for complex systems, which we can avoid in classical (Newtonian) dynamics simulations. Furthermore, a power spectral analysis with maximum entropy method [18] is used to estimate a vibrational spacing of the Auger decay spectrum.

2. Computational method

The detailed computational procedure of the density functional theory (DFT) part has already been described elsewhere [19, 20]. In short, in order to determine the absolute energy position of the excited states, normal Δ Kohn-Sham (Δ KS) calculations were performed to compute the ionization energy (IP) including full relaxation of the core-hole. The resonantly excited states were variationally determined with maintained orthogonality between the excited states through the following procedure: the first excited state was obtained by fixing the occupation of the core spin orbital to zero and placing the excited electron in the first unoccupied orbital. A full relaxation with this constraint leads to a state that is near-orthogonal to the ground state due to the $1s^{-1}$ configuration. The next state was then obtained by removing the variationally determined excited orbital from the variational space and occupying the next level. This procedure gives a variational lower bound to the energy and guarantees orthogonality between the excited states since all remaining orbitals now have to be orthogonal to the successively defined and eliminated levels [20].

In order to estimate absolute excitation energies more accurately, relativistic and functional corrections were added to the excitation energy [21]; relativistic effects on the IP of 0.18 eV for the N edge, and functional corrections to the energy of -0.06 eV for the N core excitation, where the latter value was determined by the difference between experimental and computational values of the core-ionization energy of NH₃ in the gas phase. In order to obtain an improved representation of the relaxation effects in the inner orbitals, the ionized center was described using the IGLO-III basis of Kutzelnigg et al. [22]. Gradient-corrected exchange and correlation functionals due to Perdew and Wang were applied in the present study [23, 24]. The calculations have been performed using the StoBe-DeMon program [25].

In order to consider dynamical effects in the core-excited state, CHES MD simulations were performed [9, 10, 17]. Several hundred initial structures differing from the ground state equilibrium geometry through various values of three bond lengths, two bond angles, and a dihedral angle, were sampled to determine the resulting excitation energy over the full geometrical space spanned by the initial state vibrations. The initial velocities for each atom in these starting geometries were set to zero. The time step in all CHES MD simulations was set to 0.1 fs. The Verlet integrator was applied to solve the classical equations of motion and the trajectory calculations were propagated for 30 fs.

A detailed computational procedure of Auger decay spectra has been described elsewhere [17, 26, 27]. Briefly, a set of core-hole molecular orbitals (MO's) was obtained by the above DFT calculations. A formulation can be derived in the case of resonant Auger transitions in which case the wave functions describe (N-1) electrons in the doublet Auger final state. Limited spin-symmetry-adapted configuration interaction (CI) calculations within the two-hole valence space were performed to determine the Auger final state wave functions. The Auger transition probability is approximated simply by atomic populations of valence orbitals on the excited atom while neglecting the term associated with the Auger electron. In the present study Löwdin's population analysis was adopted. CI calculations using spectator wave functions, which has two-hole and one-electron configurations, were performed. We call this as spectator Auger spectrum.

Auger decay calculations were performed for each CHES MD simulation snapshot. The theoretical spectra were constructed by convolution of the line spectra using Gaussian functions with a fixed full width at half maximum (FWHM) of 0.4 eV for the first resonant Auger spectra over the whole energy range. The final spectra were obtained by summation of spectra at 0.5 fs

time-steps from a series of trajectories weighted by the lifetime decay ratio, $\exp(-t/\tau)$, where τ is the lifetime of the core-hole; in this case 5.0 fs for the core-hole of the N atom was used, whose value is within the range of 4.7 fs for HCN [28] to 6.6 fs for N₂ [29]. In order to simulate the experimental spectra for a given excitation energy E_0 , the spectra from each trajectory were summed with a Gaussian weight [30]. For comparison with experiments we used 80 meV. The MOLYX package has been used to calculate the Auger spectra.

Although the vibrational structure of Auger decay spectra of ammonia in experiment is originated with Franck-Condon profile between the first core-excited and Auger final state, the vibrational frequencies on the core-hole state should be informative. Power spectra analyses were performed to obtain the dynamical information available from the results of CHES MD simulations. Usually, a power spectrum for a given dynamical physical property such as a coordinate or velocity can be computed by taking the Fourier transform (FT). Our problem is that the length of each CHES MD trajectory is too short, only 30 fs. The sharp peak with the ordinal FT cannot be described due to a peak broadening by the Heisenberg's uncertainty principle. We applied maximum entropy method (MEM). We call it as short-time MEM (ST-MEM) [18]. In the previous study, one of the authors found that power spectral analysis with ST-MEM was powerful tool for analyzing short-time length of trajectories such as a trajectory including a few vibrational periods. This procedure was applied to estimate the vibrational spacing for the core-excited resonant state of ammonia. Obtained peak positions should correspond to energy spacing in the vibrational progression of the experimental Auger spectra. Furthermore, the excitation energy dependent spectra can be calculated in the same analogy for the spectator Auger spectra described in the previous subsection.

3. Results and discussion

Firstly, we discuss the dissociation process on the resonant core-excited state. Elongations of a bond length X-H on the first resonant core-excited state are summarized in Table 1, where X means N for NH₃, O for H₂O, and F for HF. It is noted that these molecules are isoelectronic with neon. Although CH₄ is also the same category, it is excluded because the potential energy surface on the first resonant core-excited state is attractive. Bond lengths at the ground state shorten with increasing the atomic number in target molecules, and gradients become more negative. These are interpreted by the nuclear-nuclear repulsion between a core-hole and a hydrogen atom and by the excitation to the unoccupied orbital for the target chemical bond [27]. Bond-length elongations ΔR are about 0.2 Å for HF and H₂O and 0.046 Å for NH₃, because ΔR depends on a gradient on the core-hole state and the core-hole lifetime which decreases with

increasing nuclear charge of X. It is suggested that proton dynamics of NH_3 on the first resonant core-hole state is different with HF and H_2O .

Time propagation of X-H bonds is illustrated for each molecule during 10 fs for HF, 20 fs for H_2O , and 50 fs for NH_3 in Fig. 1(a). The starting geometry of CHES MD was the equilibrium structure at the ground state and the initial velocities of each atom were set to zero. Although 50 fs trajectory is too long compared with the core-hole lifetime of the N atom of 5.0 fs, it is valuable to see the trends of bond length elongation. For HF, an F-H bond elongates along a strong repulsive potential energy surface. For H_2O , two hydrogen atoms initially move symmetrically away from the oxygen atom, followed by one hydrogen returning to the oxygen and the other dissociating leading to bond scission into $\text{OH} + \text{H}$. For NH_3 , umbrellalike motion is excited, which is N-H symmetric stretching and bending and the motion to open the umbrella in this case. Although it is well-known that the potential energy surface along the N-H bond is repulsive [12, 8], the N-H bond rupture could not be observed due to small vibrational mode couplings. It is known that the umbrellalike motion is excited by core-excitation for AX_3 molecules [31]. It is also noted that the velocity of the N-H bond elongation is slower than O-H and F-H. Under this initial condition and during the propagating time, the N-H bond dissociation cannot be observed. In Fig. 1(b), the same trajectory to NH_3 of Fig. 1(a) and a typical trajectory using the initial N-H bond lengths different with the equilibrium at the ground state is shown, i.e., three N-H bonds set to 0.9, 1.0, and 1.0 Å, respectively. Using such an asymmetric initial geometry, a rapid N-H bond length elongation is observed. It is important to simulate molecular Auger spectra by the CHES with different initial geometry sampling [17], which we will discuss later.

Next, time propagation of the first spectator Auger spectrum of ammonia is shown in Fig. 2 together with the trajectories of the CHES MD simulations during 20 fs. Gaussian functions with an FWHM of 1.0 eV were used to convolute the line spectra. The initial structure was the optimized ground state geometry and the initial velocities were set to zero. Spectral shape of the summed spectrum in Fig. 2 is quite similar to the normal Auger spectrum of ammonia [26]. Each peak was assigned to the same way with the normal Auger spectrum except for the existence of a spectator electron. Unlike the case of water at the first core-excited state [17], mainly excited vibrational motion is the umbrellalike motion. The change in the shape of the spectra due to the time propagation is not so significant, which is similar with the case of the normal Auger spectrum of water.

In the previous report [17], one of the authors has discussed that wide range of sampling on the

ground state should be needed to reproduce the Auger spectrum of water by $O(1s) \rightarrow 4a_1$ excitation, indicating that the equilibrium structure at the ground state without the initial velocity is not good initial point. Especially the case of ammonia, an N-H bond scission may not take place with the initial geometry at the ground state equilibrium structure due to the small vibrational mode coupling as shown in Fig. 1 [12]. Furthermore, we are also interested in the excitation energy dependence of the spectator Auger spectra, which reflects on the excitation with different Franck-Condon region and derives different proton dynamics for the target molecule. To examine it theoretically, an initial geometry sampling for wide range of potential energy surface is needed. Similar scheme with the previous study was applied for the case of ammonia. Initial structures for several hundred points around the equilibrium geometry at the ground state systematically were sampled for CHES MD simulations as the starting point.

Excitation energy dependence of spectator Auger spectra of ammonia is shown in Fig. 3. Three large peaks are observed and proposed assignments are also shown. Detuning the excitation energy the shape of the spectra is not changed dramatically, suggesting that the proton motion induced by the CHES MD simulation is inefficient with the spectator Auger spectra of ammonia. N-H bond elongations within the core-hole lifetime of 5.0 fs detuning the excitation energy are shown in Table 2. The N-H bond length at 5.0 fs was obtained from the CHES MD trajectories for each sampled geometry, and summed with the Gaussian weight described above for each excitation energy E_0 . For all cases, N-H bond lengths on the core-hole state are elongated than the equilibrium bond length of the ground state. Although there is little difference of the N-H bond length after 5.0 fs, those are decreased with increasing excitation energy due to the potential energy surface on the core-hole state. Compared with the case of water [17], the bond-length variance is explicitly small. In Fig. 4 two-dimensional map of spectator Auger spectra are illustrated. Although the largest peak is slightly shifted to lower kinetic energy with increasing the excitation energy, peak positions of three main peaks are basically independent with detuning the excitation energy due to a slow dynamics on the core-hole state.

Vibrational progression was observed in the range of electron kinetic energy from 380 to 385 eV in the experiment [8], which was assigned as the fragment lines. According to the paper by Edvardsson et al. [32] the valence spectrum showed vibrational progressions in the ionic states, and the symmetric stretch mode has approximately 400 meV vibrational energy, while the bend mode has about 200 meV. Even the spectrum of the NH_2 ion has been calculated and a bend vibrational energy of about 3400 cm^{-1} was found by Stephens et al [33]. However, experimental vibrational spacing cannot connect with the fragment vibrational structure directly, because experimental vibrational structure should be due to the quantum effect such as the

Franck-Condon profile between the first core-excited and Auger final state. Our theoretical spectra cannot reproduce this structure, because our dynamical treatment depends on the classical mechanics. To induce vibrational frequencies from trajectories, power spectral analysis may be one of the solutions to obtain vibrational frequencies at the core-hole state. Obtained vibrational frequencies correspond to dynamics on the core-hole state in this analysis, not the fragment ions. Our approach is another procedure to understand the vibrational structure in the experiment. We induce the similar information using trajectories by power spectral analysis with ST-MEM [18].

ST-MEM spectra are given in Fig. 5. We will see two peaks, 340 and 450 meV, which are assigned to N-H symmetric and anti-symmetric stretching motions, respectively, by analyzing some trajectory motions. These values correspond with the experiment of 390 ± 10 meV. So we may assign the experimental vibrational spacing as N-H stretching motion. A mismatch is due to the different picture of the target physical quantity: Our values only depend on the core-hole potential energy surface, and the approach is still classical. A remarkable point is that although the explicit N-H bond dissociation is not observed during the core-hole lifetime, the vibrational spacing can be expressed using trajectories of the dynamics on the core-hole excited state. A peak of 253 meV at the detuning energy of -0.1 eV may be an unexpected noise. Vibrational modes for bending are not observed because length of trajectory is too short to recognize as the vibration.

Hjelte et al. showed that the signal attributed to ultrafast fragments is relatively weak and molecular contribution of 99.2 % is estimated dissociation lifetime as about 30 fs [8]. We also estimated the amount of molecular contribution in the Auger spectra. N-H bond dissociation threshold set to 1.5 Å, which is the same value in the case of water [17] and is also reasonable from Fig. 1 as the bond dissociation threshold. At excitation energy of 400.54 eV, product ratio of NH_3 was 99.97 % for the use of the core-hole lifetime of 5.0 fs and fragment contribution was NH_2 only, suggesting that our product ratio is reasonable to compare with the experiment. In the present study, spectator Auger spectra of ammonia were reproduced theoretically with CHES MD simulations. The vibrational spacing which is assigned as the N-H stretching motion was obtained by ST-MEM method and obtained vibrational spacing are comparable with the experiment, suggesting vibrational structures assigned with a fragment ion in reference [8] should perhaps be associated with the parent ion.

4. Summary

In the present study we performed theoretical spectator Auger spectra calculations of ammonia including the CHES MD simulations. Our theoretical Auger spectra can reproduce the experiment except for the vibrational progression assigned to fragment lines. It is necessary to emphasize that the stretching motion on the core-hole state is sensitive to the Auger spectra; on the other hand, the bending motion is insensitive. According to the CHES MD simulations, explicit bond dissociation of the N-H bond cannot be expected during core-hole lifetime of 5.0 fs due to the gentle potential energy surface along the N-H bond, which was expected from the experiment. Although the N-H bond dissociation take place slightly, only bond elongation of the N-H bond may take place at the core-hole state. Vibrational spacing was estimated using the CHES MD simulations by the ST-MEM analysis. Obtained vibrational spacing was similar with the experiment, and that vibrational mode was assigned to N-H stretching mode. We showed the results of the spectator Auger decay, which are two-hole and one electron final state. It is also interesting to examine the participator Auger decay, which are one-electron final states.

5. Acknowledgements

The authors thank Information Media Center at Hiroshima University for the use of a grid with high-performance PCs, and Research Center for Computational Science, Okazaki, Japan for the use of a Fujitsu VPP5000 and PRIMEQUEST. One of the authors (O.T.) also acknowledges useful discussion with Dr. H. Yoshida from Hiroshima University.

Table 1 Gradient of potential energy surface on the core-hole state and X-H bond elongation within core-hole lifetime for HF, H₂O, and NH₃.

Molecule	R(X-H)(eq.) ^(a) / Å	Gradient / eV Å ⁻¹	ΔR ^(b) / Å
HF	0.92	-13.75	0.23
H ₂ O	0.98	-4.50	0.19
NH ₃	1.01	-3.13	0.046

^(a) Equilibrium bond length at the ground state for X-H bond, where X means F, O, and N atoms, respectively.

^(b) Bond elongation within core hole lifetime (2.0 fs for F(1s), 4.1 fs for O(1s), and 5.0 fs for N(1s)) during CHES MD calculations.

Table 2 N-H bond-length elongation (in Å) within a core-hole lifetime of 5.0 fs^(a).

Excitation energy (eV)	Bond length (Å)
400.44	1.065
400.54	1.054
400.64	1.045

^(a) N-H bond length at the equilibrium is 1.010 Å.

Figure captions

Fig. 1 Time propagation of X-H bond lengths, where X is F for HF, O for H₂O, and N for NH₃ respectively, by CHES MD simulations during 20 fs for the first resonant core-excited state. Trajectories for each molecule are also shown. (a) In the case of HF and H₂O. Initial geometries set to the equilibrium geometry at the ground state. CHES MD simulations during only 10 fs for HF and during 50 fs for NH₃ are illustrated. (b) In the case of NH₃. Green lines indicate NH bond lengths where the initial geometry set to the ground state equilibrium geometry, and blue lines indicate typical asymmetric initial bond lengths, i.e., three N-H bonds set to 0.9, 1.0, and 1.0 Å respectively, are used as the initial geometry.

Fig. 2 Time propagation of the spectator Auger spectra by CHES MD simulations of ammonia. Summed weighted spectra and a trajectory of this simulation during 20 fs are also shown. Gaussian functions with a FWHM of 1.0 eV were used to convolute the line spectra. The initial geometry is the ground state equilibrium structure.

Fig. 3 Spectator Auger spectra of ammonia following N(1s)→4a₁ excitation. The detuning is relative to the center of the N(1s)→4a₁ absorption resonance (400.54 eV). Main configurations of peaks are also shown.

Fig. 4 Two-dimensional contour map of spectator Auger spectra of ammonia following N(1s)→4a₁ excitation. Peak intensity represents the color legend from blue to red in arbitrary units.

Fig. 5 ST-MEM spectra of ammonia following N(1s)→4a₁ excitation. The detuning is relative to the center of the N(1s)→4a₁ absorption resonance (400.54 eV).

Figure 1

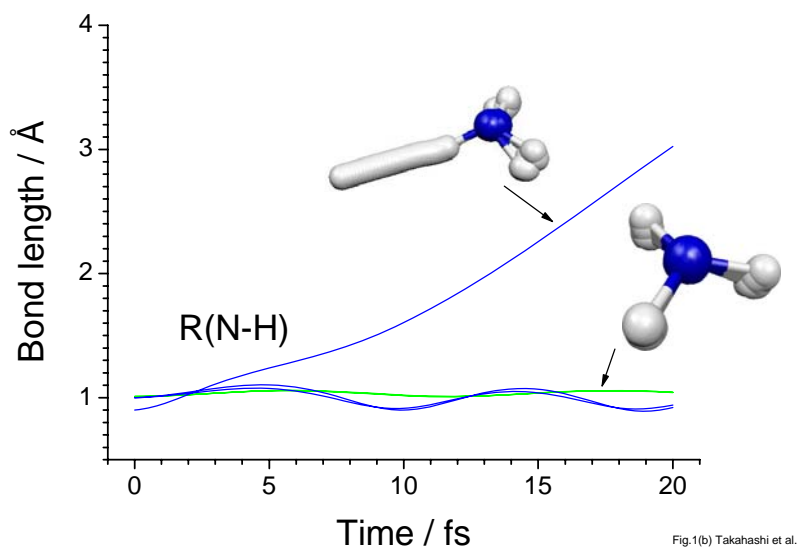
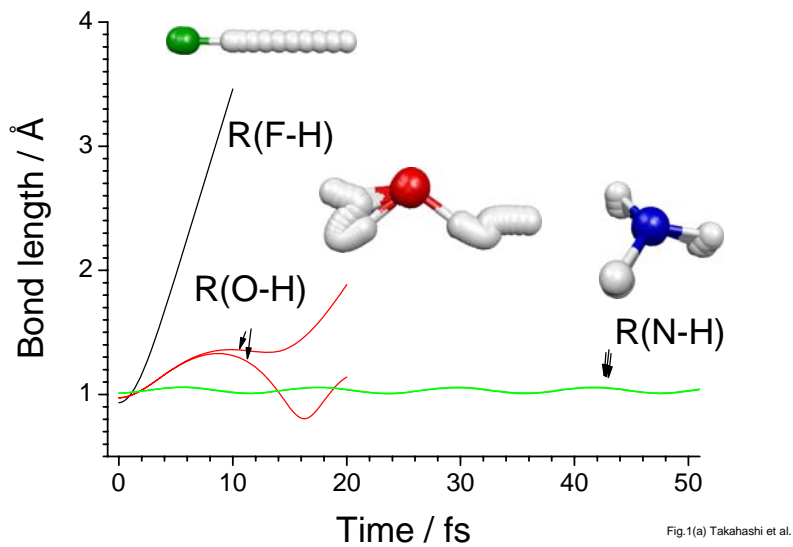


Figure 2

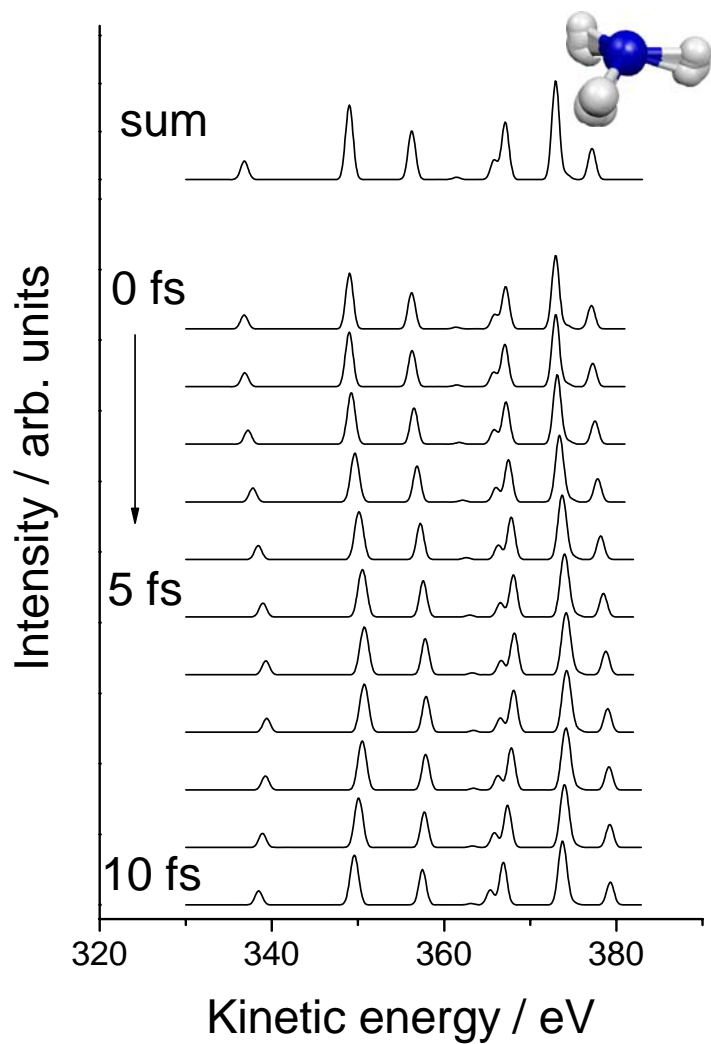


fig.2 Takahashi et al

Figure 3

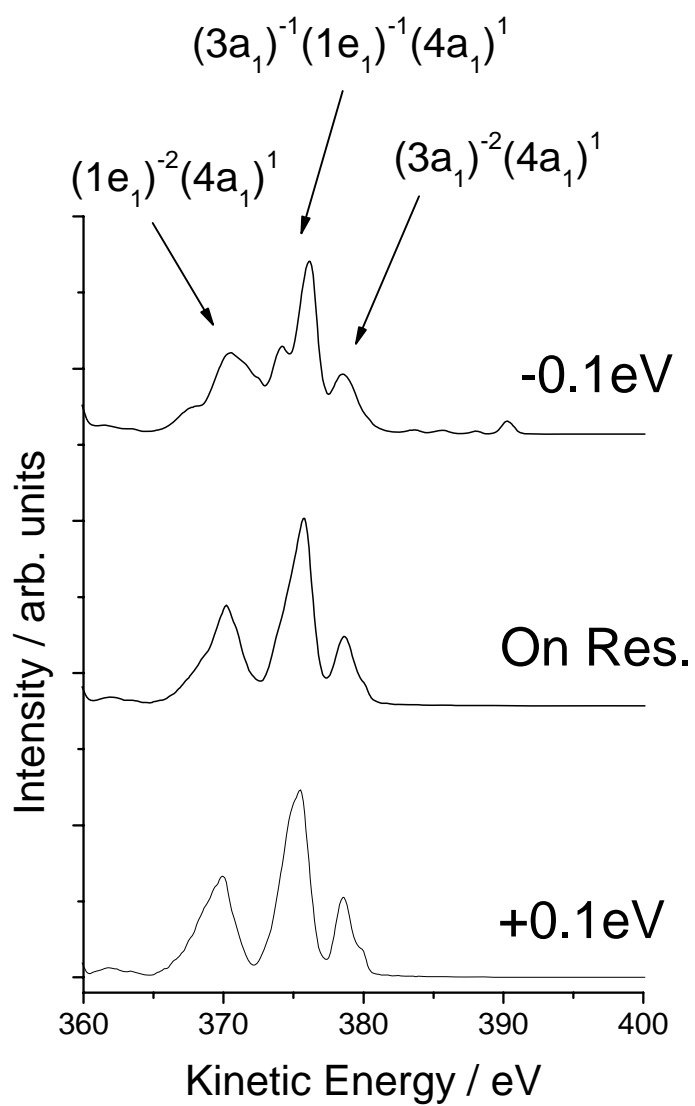


Fig.3 Takahashi et al

Figure 4

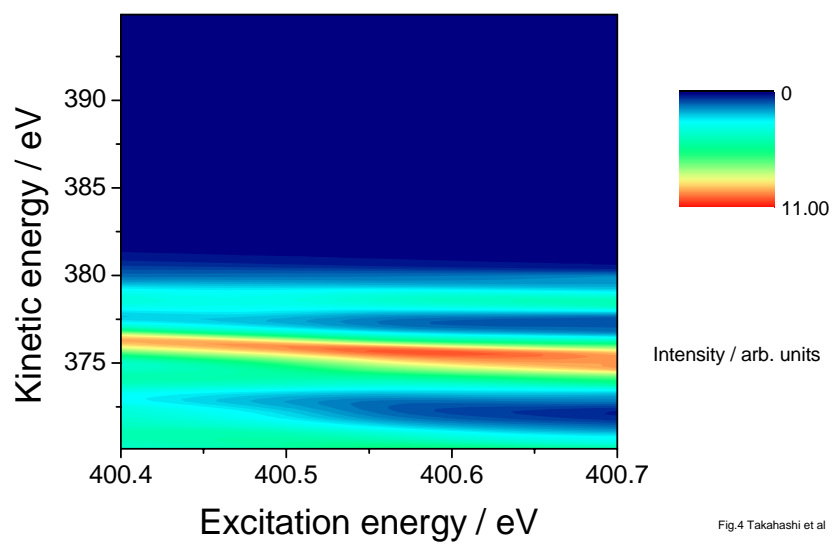
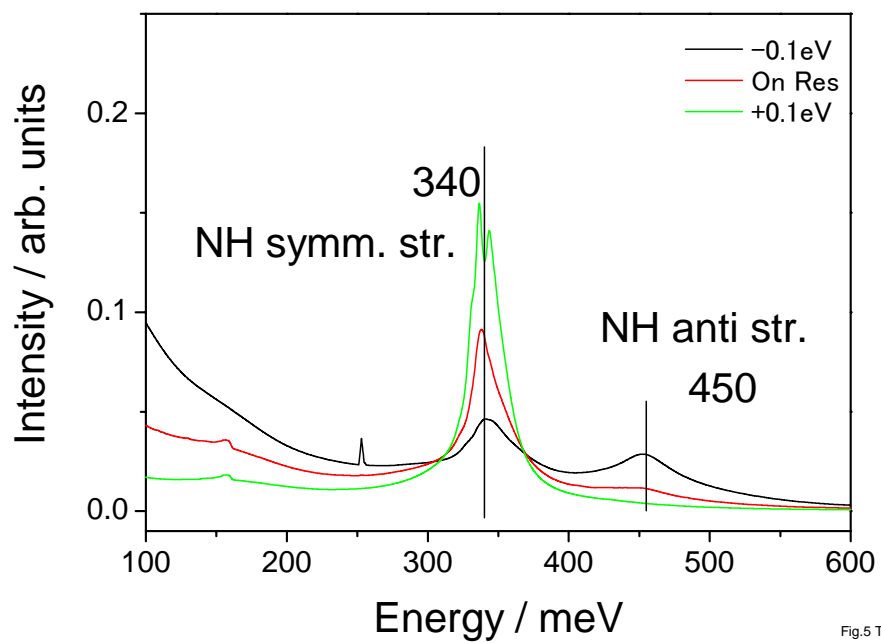


Figure 5



References

- [1] Mehlhorn W 1998 *J. Electron. Spectrosc. Relat. Phenom.* **93** 1-15
- [2] Piancastelli M N 2000 *J. Electron. Spectrosc. Relat. Phenom.* **107** 1-26
- [3] Morin P and Nenner I 1986 *Phys. Rev. Lett.* **56** 1913-6
- [4] Björneholm O, Sundin S, Svensson S, Marinho R R T, Naves de Brito A, Gel'mukhanov F and Ågren H 1997 *Phys. Rev. Lett.* **79** 3150-3
- [5] Aksela H, Aksela S, Ala-Korpela M, Sairanen O P, Hotokka M, Bancroft G M, Tan K H and Tulkki J 1990 *Phys. Rev. A* **41** 6000-5
- [6] Naves de Brito A, Feifel R, Mocellin A, Machado A B, Sundin S, Hjelte I, Sorensen S L and Björneholm O 1999 *Chem. Phys. Lett.* **309** 377-85
- [7] Hjelte I, Piancastelli M N, Fink R F, Björneholm O, Bäsler M, Feifel R, Giertz A, Wang H, Wiesner K, Ausmees A, Miron C, Sorensen S L and Svensson S 2001 *Chem. Phys. Lett.* **334** 151-8
- [8] Hjelte I, Piancastelli M N, Jansson C M, Wiesner K, Björneholm O, Bassler M, Sorensen S L and Svensson S 2003 *Chem. Phys. Lett.* **370** 781-8
- [9] Brena B, Nordlund D, Odelius M, Ogasawara H, Nilsson A and Pettersson L G M 2004 *Phys. Rev. Lett.* **93** 148302-4
- [10] Odelius M, Ogasawara H, Nordlund D, Fuchs O, Weinhardt L, Maier F, Umbach E, Heske C, Zubavichus Y, Grunze M, Denlinger J D, Pettersson L G M and Nilsson A 2005 *Phys. Rev. Lett.* **94** 227401-4
- [11] Alagia M, Baldacchini C, Betti M G, Bussolotti F, Carravetta V, Ekstrom U, Mariani C and Stranges S 2005 *J. Chem. Phys.* **122** 124305-6
- [12] Schirmer J, Trofimov A B, Randall K J, Feldhaus J, Bradshaw A M, Ma Y, Chen C T and Sette F 1993 *Phys. Rev. A* **47** 1136-47
- [13] Senba Y, Goya T, Yoshida H and Hiraya A 2005 *J. Electron. Spectrosc. Relat. Phenom.* **144-147** 195-7
- [14] Lindgren A, Gisselbrecht M, Burmeister F, Naves de Brito A, Kivimaki A and Sorensen S L 2005 *J. Chem. Phys.* **122** 114306-9
- [15] Piancastelli M N, Guillemin R, Stolte W C, Ceolin D and Lindle D W 2007 *J. Electron. Spectrosc. Relat. Phenom.* **155** 86-90
- [16] Lindblad A, Bergersen H, Pokapanich W, Tchapyguine M, Öhrwall G and Björneholm O 2009 *Phys. Chem. Chem. Phys.* **11** 1758-64
- [17] Takahashi O, Odelius M, Nordlund D, Nilsson A, Bluhm H and Pettersson L G M 2006 *J. Chem. Phys.* **124** 064307-9

- [18] Takahashi O, Nomura T, Tabayashi K and Yamasaki K 2008 *Chem. Phys.* **351** 7-12
- [19] Triguero L, Pettersson L G M and Ågren H 1998 *Phys. Rev. B* **58** 8097-110
- [20] Kolczewski C, Püttner R, Plashkevych O, Ågren H, Staemmler V, Martins M, Snell G, Schlachter A S, Sant'Anna M, Kaindl G and Pettersson L G M 2001 *J. Chem. Phys.* **115** 6426-37
- [21] Takahashi O and Pettersson L G M 2004 *J. Chem. Phys.* **121** 10339-45
- [22] Kutzelnigg W, Fleischer U and Schindler M 1990 *NMR-Basic Principles and Progress* (Heidelberg: Springer-Verlag)
- [23] Perdew J P and Yue W 1986 *Phys. Rev. B* **33** 8800-2
- [24] Perdew J P and Wang Y 1992 *Phys. Rev. B* **45** 13244-9
- [25] Hermann K, Pettersson L G M, Casida M E, Daul C, Goursot A, Koester A, Proynov E, St-Amant A, Salahub D R, Carravetta V, Duarte H, Friedrich C, Godbout N, Guan J, Jamorski C, Leboeuf M, Leetmaa M, Nyberg M, Patchkovskii S, Pedocchi L, Sim F, Triguero L and Vela A 2006 StoBe-deMon Version 2.2.
- [26] Mitani M, Takahashi O, Saito K and Iwata S 2003 *J. Electron. Spectrosc. Relat. Phenom.* **128** 103-17
- [27] Takahashi O, Matsui T, Kawano A, Tabayashi K and Yamasaki K 2007 *J. Mol. Struct. Theochem* **808** 35-40
- [28] Giertz A, Børve K J, Bäßler M, Wiesner K, Svensson S, Karlsson L and Sæthre L J 2002 *Chem. Phys.* **277** 83-90
- [29] Hergenhahn U, Kugeler O, Rudel A, Rennie E E and Bradshaw A M 2001 *J. Phys. Chem. A* **105** 5704-8
- [30] Stöhr J 1992 *NEXAFS Spectroscopy* (Berlin: Springer-Verlag)
- [31] Ekström U, Carravetta V, Alagia M, Lavollee M, Richter R, Bolcato C and Stranges S 2008 *J. Chem. Phys.* **128** 044302-11
- [32] Edvardsson D, Baltzer P, Karlsson L, Wannberg B, Holland D M P, Shaw D A and Rennie E E 1999 *Journal of Physics B: Atomic, Molecular and Optical Physics* 2583
- [33] Stephens J C, Yamaguchi Y, Sherrill C D and Schaefer H F 1998 *The Journal of Physical Chemistry A* **102** 3999-4006